BEARING CAPACITY DETERMINATION BY LIMIT ANALYSIS

by

Wai F. Chen

Hugh L. Davidson

Fritz Engineering Laboratory
Department of Civil Engineering
Lehigh University
Bethlehem, Pennsylvania

January 1972

Fritz Engineering Laboratory Report No. 355.15

BEARING CAPACITY DETERMINATION BY LIMIT ANALYSIS

by

Wai F. Chen[1] and Hugh L. Davidson[2]

Key Words: Bearing capacity, Cohesive soils, Failure, Limit analysis, Plasticity, Soil mechanics, Stability, Upper bound

ABSTRACT: The upper bound technique of limit analysis is used to develop approximate solutions for the bearing capacity of cohesive soils with weight. Solutions are presented for smooth and rough and surface and subsurface footings. Soil is treated as a perfectly plastic medium with the associated flow rule after Drucker. The limit analysis solutions for smooth, surface footings are shown to compare favorably with slip-line solutions. Meyerhof's solutions and the limit analysis solutions for rough, subsurface footings are shown to agree remarkably well.

[1]Associate Professor of Civil Engineering, Fritz Laboratory, Lehigh University, Bethlehem, Pa.
[2]Teaching Assistant, Department of Civil Engineering, Lehigh University, Bethlehem, Pa.

TABLE OF CONTENTS

		Page
	ABSTRACT	i
1.	INTRODUCTION	1
2.	LIMIT ANALYSIS, SLIP-LINE AND LIMIT EQUILIBRIUM METHODS	3
3.	GOVERNING PARAMETERS	6
4.	UPPER BOUND SOLUTIONS OF THE BEARING CAPACITY PROBLEM	6
5.	NUMERICAL SOLUTIONS	12
6.	RESULTS AND DISCUSSION	13
7.	COMPARISON OF RESULTS WITH EXISTING SOLUTIONS	16
8.	SUMMARY AND CONCLUSIONS	19
	APPENDIX 1 - REFERENCES	20
	APPENDIX 2 - BEARING CAPACITY OF COHESIONLESS SOILS	22
	APPENDIX 3 - NOTATION	23
	TABLES	25
	FIGURES	28
	ACKNOWLEDGEMENTS	42

1. INTRODUCTION

This paper presents an approximate solution technique and solutions for the two-dimensional bearing capacity problem. Since approximate solutions for bearing capacity abound, one might question the need for a new set of approximate answers. Neither the failure mechanisms nor the solutions presented here are radically different from what has been presented in the past. However, the method is rational and completely self-consistent, being based on a few well-defined assumptions. It admits a closed form expression for the bearing capacity in terms of the governing parameters of the problem and the geometry of the failure mechanism. It also provides engineers with a clear physical picture of the mode of failure and can be easily utilized by the engineer as a working tool to obtain particular solutions he needs for his problem. The method can be readily applied to both smooth and rough footings and to surface and subsurface footings. In addition there is no need to use "superposition" as is commonly employed in the so-called limit equilibrium method.

The problem considered here is that of a rigid punch bearing on an infinite half-space of isotropic homogeneous soil. The soil will be assumed to be in a state of plane strain and the base of the punch may be either smooth or rough.

Soil is modeled here as elastic-perfectly plastic material obeying the Coulomb yield condition. All displacements are assumed to be small. If the material is assumed to deform according to the flow rule associated with the Coulomb yield condition [5], then the

powerful bounding theorems of limit analysis can be utilized [5]. However, the physical validity of this flow rule is questionable [1]. An upper bound obtained with this assumption is an upper bound for a frictional material, but lower bounds have a less definite meaning [4]. It should further be noted that if finite but non-zero friction is assigned to the footing base or walls, limit analysis techniques do not produce rigorous upper or lower bounds [4]. Since stress fields are not considered here, solutions obtained from the velocity fields or failure mechanisms can at best give only upper bounds to the true bearing capacity. However, it is shown in what follows that the upper bound technique of limit analysis will yield good answers to the bearing capacity problem when compared with existing exact solutions.

Studies of the bearing capacity of foundations under conditions of plane strain have been made by Terzaghi [20], by Meyerhof [12], by Sokolovskii [18], by Hansen [9], by Shield [16], by Cox [2], and many others. Some of the information to be presented here is contained, therefore, in this previous work but the relevant parts of each have not yet been compared in principal. Although all the analyses utilize the concept of perfect plasticity, the relation between these solutions, corresponding to different analytical methods, involves terminology and special concepts that are not in common use in the field of soil mechanics. A brief description of the salient features of these methods will therefore be given.

These methods, discussed in the following section, are limit analysis, slip-line method, and limit equilibrium.

2. LIMIT ANALYSIS, SLIP-LINE AND LIMIT EQUILIBRIUM METHODS

For an elastic-perfectly plastic material with the associated flow rule, Drucker, Prager, and Greenberg [6] have developed upper and lower bound limit theorems which allow one to bound the true ultimate load (or plastic limit load). The computation of such bounds is generally referred to as limit analysis.

The lower bound theorem of limit analysis states that if a distribution of stress, over the domain in question, can be found which satifies the equations of equilibrium, the stress boundary conditions and the yield condition, the load associated with this stress distribution is less than or at best equal to the true ultimate load or limit load.

The upper bound theorem of limit analysis states that if the power of the external load is greater than or equal to the rate of internal energy dissipation associated with a kinematically admissible velocity field, then the load must be greater than or at best equal to the true ultimate or limit load. If the upper and lower bounds coincide, the limit load is the true collapse load.

The upper bound technique of limit analysis is employed here to generate approximate solutions to the bearing capacity problem. The lower bound technique of limit analysis is not considered but the computer method presented by Lysmer [11] can be applied and may give good lower bound solutions.

The term slip-line method refers to the integration of the characteristic stress equations of the plastic equilibrium field. The numerical solution of these characteristic equations is described in detail by Sokolovskii [18]. Josselin De Jong has described a graphical method of solution [3]. The slip-line method yields a plastic equilibrium stress field around the foundation, however, there is no guarantee that this stress field can be extended satisfactorily throughout the body, nor is it necessarily possible to associate velocity fields with these stress fields. A slip-line solution for the bearing capacity of a foundation is therefore not necessarily the true solution nor is it known when it is an upper bound or a lower bound solution. If one employs the associated flow rule and can integrate the resulting stress-strain rate equations to yield a kinematically admissible velocity field, the slip-line solution is an upper bound solution. If, in addition, the slip-line stress field can be extended over the entire soil domain (usually an infinite half-space) such that the equilibrium equations, the stress boundary conditions and the yield condition are satisfied, the slip-line solution is also a lower bound and is hence the true solution.

Slip-line solutions that have not been shown to be lower bounds are usually referred to as incomplete solutions. Those which have been shown to be lower bounds are referred to as complete solutions. The Prandtl [14] solution for the bearing capacity of a surface footing resting on a cohesive weightless soil, for example, has been shown by Shield [17] to be complete. The few slip-line solutions for soils with weight are as yet incomplete, although it is commonly assumed,

at least for smooth footings, that it will be possible to show them to be complete (for instance see Ref. 2, page 380).

Although the slip-line method can generally be expected to give a good estimate of the correct solution, closed form solutions can only be obtained for weightless soils. The characteristic equations must be integrated numerically or graphically if soil weight is included in the analysis. To date this has only been done for the simple geometries.

The so-called limit equilibrium or plastic equilibrium method has traditionally been used to obtain approximate solutions for the bearing capacity of soils. Examples of this approach are the solutions of Terzaghi [20] and Meyerhof [12]. The method can probably best be described as an approximate approach to the construction of a slip-line field and generally entails an assumed failure surface. It is necessary to make sufficient assumptions about the stress distribution within the soil domain bounded by the failure surface such that an equation of equilibrium, in terms of resultant forces, may be written for the bearing capacity determination.

None of the equations of continuum mechanics are explicitly satisfied everywhere inside or outside of the failure surface. Since the stress distribution is not defined precisely everywhere inside of the assumed failure surface, one can not say definitely that a stress distribution compatible with the assumed failure surface and satisfying equilibrium, stress boundary conditions and the yield function exists. Although the limit equilibrium technique utilizes the

basic philosophy of the upper bound theorem of limit analysis, that is, a failure surface is assumed and a least answer is sought, it is not an upper bound. The method basically gives no consideration to soil kinematics, and equilibrium conditions are satisfied only in a limited sense.

It is clear then that a solution obtained using the limit equilibrium method is not necessarily an upper or a lower bound. However, any upper bound limit analysis solution will obviously be a limit equilibrium solution.

3. GOVERNING PARAMETERS

Cox [2] has shown that for a smooth surface footing bearing on a soil subjected to no surcharge, the fundamental dimensionless parameters associated with the stress characteristic equations are ϕ and $G = \gamma B/2c$, where φ is the internal friction angle, c is the cohesive strength, γ is the unit weight of soil and B is the width of the footing. If G is small the soil behaves essentially as a cohesive weightless medium. If G is large soil weight rather than cohesion is the principal source of bearing strength. For most practical cases one can expect that G will range from .1 to 1.0. These limits assume that c ranges from 500 psf to 1000 psf, and that the footing width ranges from 3 to 10 feet.

4. UPPER BOUND SOLUTIONS OF THE BEARING CAPACITY PROBLEM

Two distinct velocity fields, referred to here as the Prandtl

and Hill mechanisms, were utilized in the analysis. In this paper the terms "mechanism" and "velocity field" will be used interchangeably.

The Prandtl mechanism, consisting of three zones, is shown diagramatically in Fig. 1. The wedge, ABC, is translating vertically as a rigid body with the same initial downward velocity V_1 as the footing. The downward movement of the footing and wedge is accommodated by the lateral movement of the adjacent soil as indicated by the radial shear zone BCD and zone BDEF. The angles ξ and η are as yet unspecified. Since the movement is symmetrical about the footing, it is only necessary to consider the movement on the right-hand side of Fig. 1. The radial shear zone BCD may be considered to be composed of a sequence of rigid triangles as shown in the left-hand side of Fig. 1 [1]. All the small triangles and the zone BDEF move as rigid bodies in directions which make an angle φ with the discontinuity lines CD and DE respectively. The velocity of each small triangle is determined by the condition that the relative velocity between the triangles in contact must have the direction which makes an angle φ to the contact surface. It is found that the velocity for each triangle is $V = V_o \exp(\theta \tan\varphi)$ [1]. The velocity V_3 in the zone BDEF is perpendicular to the radial line BD. Hence, the velocity field is continuous across line BD. Line DE is constrained to be tangent to the log spiral curve at point D.

Energy is dissipated at the discontinuity surfaces between the material at rest and the material in motion and at the discontinuity surfaces between adjacent rigid bodies. It is a simple matter to calculate the lengths of the lines of discontinuity. The rate of energy

dissipation is then found by multiplying the length of each discontinuity line by c times the velocity difference across the line multiplied by $\cos\varphi$, and summing over all such lines. For the radial shear zone BCD, it is found that as the number of rigid triangles approaches infinity, the total rate of energy dissipated within the shear zone is

$$\dot{D} = \frac{1}{2}\, c\, V_o\, r_o\, \frac{\exp(2\Theta\tan\phi) - 1}{\tan\phi} \tag{1}$$

The rate at which work is done by the soil weight is found by multiplying the area of each rigid body by γ times the vertical component of the velocity of the rigid body and summing over all the areas in motion. For the radial shear zone BCD, it is found that the total rate of external work done by the soil weight is

$$\dot{W} = \frac{\gamma r_o^2\, V_o}{2(9\tan^2\phi+1)} \left\{\exp(3\Theta\tan\phi)\,[3\tan\phi\cos(\xi+\Theta)+\sin(\xi+\Theta)] - [3\tan\phi\cos\xi+\sin\xi]\right\} \tag{2}$$

Equating the total rate at which work is done by the force on the foundation and the soil weight in motion to the total rate of energy dissipation along the lines of velocity discontinuity, it is found, after some simplification, that an upper bound on the average bearing capacity of the soil is

$$q_o/c = \tan\xi + \frac{\cos(\xi-\phi)}{\cos\xi\sin\phi}\left\{\exp[2(\pi+\beta-\eta-\xi)\tan\phi] - 1\right\} + \frac{\cos(\xi-\phi)\sin\eta\exp[2(\pi+\beta-\eta-\xi)\tan\phi]}{\cos(\phi+\eta)\cos\xi}$$

$$+ G\left[\frac{-\tan\xi}{2} + \frac{.5\cos(\xi-\phi)}{\cos^2\xi\cos\phi(9\tan^2\phi+1)}\left\{\exp(3[\pi+\beta-\eta-\xi]\tan\phi)[3\tan\phi\cos(\beta-\eta)\right.\right.$$

$$+ \sin(\beta-\eta)] + 3\tan\phi\cos\xi + \sin\xi\Big\} + \frac{\cos(\xi-\phi)\sin\eta\cos(\beta-\eta)\exp[2(\pi+\beta-\eta-\xi)\tan\phi](D/B)}{\cos\xi\cos\phi\sin\beta}$$

$$+ \frac{2\cos(\xi-\phi)\cos(\beta-\eta)\exp[(\pi+\beta-\eta-\xi)\tan\phi](D/B)^2}{\cos\phi\tan\beta}\Bigg] \qquad (3)$$

where β is related to D/B, η and ξ by the transcendental equation,

$$\sin\beta\exp(\beta\tan\phi) = \frac{2(D/B)\cos\xi\cos(\phi+\eta)}{\exp[(\pi-\eta-\xi)\tan\phi]\cos\phi} \qquad (4)$$

The best upper bound from Eq. 3 is found by minimizing function q_o/c with respect to variables ξ and η for the given values φ, G and D/B. The numerical solution of equations (3) and (4) can be obtained by the simultaneous application of the method of steepest descent for the optimum value of equation (3) and a Newton-Raphson iteration on equation (4) for angle β. The complete presentation of results and comparisons with various existing solutions will be discussed in later sections.

For the special case of a surface footing for which both D/B and β are equal to zero, Eq. 3 reduces to

$$q_o/c = \tan\xi + \frac{\cos(\xi-\phi)\{\exp[2(\pi-\eta-\xi)\tan\phi]-1\}}{\cos\xi\sin\phi} + \frac{\cos(\xi-\phi)\sin\eta\exp[2(\pi-\eta-\xi)\tan\phi]}{\cos\xi\cos(\phi+\eta)}$$

$$+ G\Bigg[\frac{-\tan\xi}{2} + \frac{.5\cos(\xi-\phi)}{\cos^2\xi\cos\phi(9\tan^2\phi+1)}\Big\{\exp[3(\pi-\eta-\xi)\tan\phi][3\tan\phi\cos\eta-\sin\eta]$$

$$+ 3\tan\phi\cos\xi + \sin\xi\Big\} + \frac{.5\cos(\xi-\phi)\sin\eta\cos\eta\exp[3(\pi-\eta-\xi)\tan\phi]}{\cos^2\xi\cos(\phi+\eta)}\Bigg] \qquad (5)$$

For a surface footing, the optimum value of η is found to be, as expected,

$$\eta = 45^o - \phi/2 \qquad (6)$$

Although the optimum value of ξ depends on G, the minimum values of the bearing capacities may be approximated to within 5 percent by using the following approximated equations,

$$\xi = 45^{o} + \phi/2 \qquad \text{if } G \leq .1 \tag{7}$$

$$\xi = \phi + 15^{o} \qquad \text{if } G > .1 \tag{8}$$

Since the kinematically admissible velocity field used in the Prandtl mechanism is such that no slip occurs between the foundation and the soil, the upper bound obtained is applicable to either a rough or a smooth footing. A better upper bound for the case of small base friction and large values of G is obtained using the Hill mechanism shown in Fig. 2. Excepting the area directly below the base, the Hill mechanism closely resembles the Prandtl mechanism. Considering now the right half of the symmetric velocity field, wedge ABC is translating as a rigid body with a downward velocity V_1 inclined at an angle φ to the discontinuity line AC. Since the soil must remain in contact with the footing, the footing must move with the downward velocity $V_1 \sin(\zeta - \varphi)$. The rest of the mechanism is similar in form to the Prandtl mechanism. Energy is dissipated along the lines AC, BC, and DE, and curve CD. Energy is also dissipated within the radial shear zone.

Since the Hill mechanism admits sliding between the footing base and the adjacent soil, dissipation of energy due to friction on this surface should be taken into account in the computation of the bearing capacity of the footing. The rate of dissipation of energy due to friction may be computed by multiplying the discontinuity in velocity $V_1 \cos(\zeta - \varphi)$ across the base surface by $\tan\delta$ (δ is the friction

angle between the base and the adjacent soil) times the normal force $q_o B$ acting on this surface. The total rate of dissipation of energy is then obtained by adding this additional dissipation to all previous dissipations. Since the soil is moving away from the footing wall BF, no frictional energy is dissipated along the wall. Equating the external rate of work done by the force acting on the footing and the weight of soil in motion to the total internal rate of energy dissipation, it is found that the value of the upper bound on the average bearing pressure is

$$q_o/c = \left[\frac{1}{1-\tan\delta\cot(\zeta-\phi)}\right] g(\xi,\eta,\zeta) \tag{9}$$

where

$$g(\xi,\eta,\zeta) = \frac{\sin\xi\cos\phi}{\sin(\zeta+\xi)\sin(\zeta-\phi)} + \frac{\text{abs}[\cos(\xi+\zeta-\phi)]\sin\zeta}{\sin(\zeta-\phi)\sin(\zeta+\xi)}$$

$$+ \frac{\alpha\sin\zeta\{\exp[2(\pi+\beta-\eta-\xi)\tan\phi] - 1\}}{\sin(\zeta+\xi)\sin\phi\sin(\zeta-\phi)} + \frac{\alpha\sin\eta\sin\zeta\exp[2(\pi+\beta-\eta-\xi)\tan\phi]}{\cos(\phi+\eta)\sin(\zeta+\xi)\sin(\zeta-\phi)} + c\left[\frac{-.5\sin\zeta\sin\xi}{\sin(\zeta+\xi)}\right.$$

$$+ \frac{.5\alpha\sin^2\zeta}{\sin^2(\zeta+\xi)\cos\phi\sin(\zeta-\phi)(9\tan^2\phi+1)}\{\exp[3(\pi+\beta-\eta-\xi)\tan\phi][3\tan\phi\cos(\beta-\eta)$$

$$+ \sin(\beta-\eta)] + 3\tan\phi\cos\xi + \sin\xi\} + \frac{\alpha\sin\zeta\sin\eta\cos(\beta-\eta)\exp[2(\pi+\beta-\eta-\xi)\tan\phi](D/B)}{\sin(\zeta+\xi)\cos\phi\sin(\zeta-\phi)\sin\beta}$$

$$\left. + \frac{2\alpha\cos(\beta-\eta)\exp[(\pi+\beta-\eta-\xi)\tan\phi](D/B)^2}{\tan\delta\cos\phi\sin(\zeta-\phi)}\right] \tag{10}$$

where $\alpha = \sin(\xi+\zeta-2\phi)$ (11)

if $-\pi/2+\xi+\zeta-\phi > 0$ (12)

otherwise $\alpha = \sin(\xi+\zeta)$ (13)

and the corresponding governing equation for β is

$$\sin\beta\exp(\beta\tan\phi) = \frac{2(D/B)\sin(\zeta+\xi)\cos(\phi+\eta)}{\sin\zeta\cos\phi\exp[(\pi-\eta-\xi)\tan\phi]} \tag{14}$$

The amplification factor $1/[1-\tan\delta\cot(\zeta-\varphi)]$ appearing in the right-hand side of Eq. 9 is contributed by the sliding friction. Minimization of the function q_o/c will be discussed later.

For the special case of a surface footing, the function $g(\xi,\eta,\zeta)$ reduces to

$$g(\xi,\eta,\zeta) = \frac{\sin\xi\cos\phi}{\sin(\zeta+\xi)\sin(\zeta-\phi)} + \frac{\sin\zeta\,\mathrm{abs}[\cos(\xi-\zeta-\phi)]}{\sin(\zeta+\xi)\sin(\zeta-\phi)}$$

$$+ \frac{\alpha\sin\zeta\{\exp[2(\pi-\eta-\xi)\tan\phi]-1\}}{\sin(\zeta+\xi)\sin\phi\sin(\zeta-\phi)} + \frac{\alpha\sin\zeta\sin\eta\exp[2(\pi-\eta-\xi)\tan\phi]}{\cos(\phi+\eta)\sin(\zeta+\xi)\sin(\zeta-\phi)} + G\left[\frac{-.5\sin\zeta\sin\xi}{\sin(\zeta+\xi)}\right.$$

$$+ \frac{.5\alpha\sin^2\zeta}{\sin^2(\zeta+\xi)\cos\phi\sin(\zeta-\phi)(9\tan^2\phi+1)}\Big\{\exp[3(\pi-\eta-\xi)\tan\phi][3\tan\phi\cos\eta-\sin\eta]$$

$$\left.+ 3\tan\phi\cos\xi + \sin\xi\Big\} + \frac{.5\alpha\sin^2\zeta\sin\eta\cos\eta\exp[3(\pi-\eta-\xi)\tan\phi]}{\sin^2(\zeta+\xi)\sin(\zeta-\phi)\cos(\phi+\eta)}\right] \qquad (15)$$

As was the case for the Prandtl mechanism, the optimum value of η for a surface footing is again found to be

$$\eta = 45^o - \phi/2 \qquad (16)$$

and the optimum values for the parameters ξ and ζ are found to satisfy the condition

$$\xi + \zeta = 90^o + \phi \qquad (17)$$

This implies that line AC is tangent to the log spiral curve at point C (referring to Fig. 2). For a smooth footing, bearing capacities can generally be approximated to within 10 percent of the minimum if

$$\xi = 45^o + \phi/2 \qquad (18)$$

5. NUMERICAL SOLUTION

In order to find the values of the mechanism parameters

that minimize the bearing capacity of footings, a modified form of the method of steepest descent was used. The optimum mechanism parameter set is found through a sequence of incremental steps, starting with an assumed set of values. The length of the incremental parameter vector is arbitrarily assigned and its direction is defined by the negative of the function gradient. After each change in the mechanism parameter vector, the load associated with this new set is compared with the old load associated with the previous parameter set. If the new load is less than the old load a new parameter set is computed, if not, the process is terminated or a new smaller incremental vector length is assigned.

The minimization procedure has been programmed for a CDC 6400 computer. Incremental vector lengths of five degrees and subsequently one degree were used in the program. Optimum values so obtained have been compared to those obtained by tabulating the function and finding the minimum by hand. Excellent agreement was observed in every case checked. Optimum values were in most cases obtained within fifteen cycles. For each new set of given conditions (ϕ, G, D/B, δ), the minimization procedure took about one-tenth of a second of computer time.

6. RESULTS AND DISCUSSION

Charts relating bearing capacity to the various governing parameters are presented in Figs. 3 to 9. Results for surface footings will be first discussed followed by a discussion of the results for shallow and deep footings.

Bearing capacities of surface footings are shown in Figs. 3 and 4. In Fig. 3 the relationship between the nondimensionalized bearing capacity, q_o/c, and the parameter G is shown for both perfectly smooth and perfectly rough footings. Soil internal friction angles ranging from five to forty-five degrees are considered. The charts clearly show that base friction has little effect upon bearing capacity for small values of G. This is to be expected since Prandtl's solution for weightless soil is independent of base friction. However, for relatively large values of G, base friction has a significant effect on bearing capacity. For instance, letting G = 10 and $\phi = 30^o$, the bearing capacity of a rough footing is approximately twice that of a smooth footing. In general the Prandtl mechanism gives the lesser upper bound for rough footings while the Hill mechanism gives the smaller bound for smooth footings. However, if G is large and $\phi \leq 5^o$, the Hill mechanism gives a lower value than the Prandtl mechanism, for rough as well as smooth footings.

The effect of base friction on the bearing capacity of footings is shown in Fig. 4. The curves are characterized by a rising portion followed by a flat plateau. At the intersection of the rising portion and the plateau the base friction is just sufficient to restrain any sliding motion between the base and the adjacent soil. Any increase then in the base friction angle will yield no increase in the bearing capacity. The results presented here indicate that a rather modest value of base friction (less than fifteen degrees for all ϕ) is sufficient to create an essentially perfectly rough condition. For ϕ greater than or equal to 10 degrees, the rising portion of the curve

is associated with the Hill mechanism while the flat plateau is associated with the Prandtl mechanism. For $\phi \leq 5^{o}$, the entire curve is obtained from the Hill mechanism.

The results for shallow and deep rough footings are presented in Figs. 5 to 8. In Figs. 5 and 6 bearing capacity is plotted against depth to breadth ratios (D/B) ranging from 0 to 1 and 0 to 10 respectively, while G = 0 and 10 and ϕ ranges from 5^{o} to 45^{o}.

The charts show that the increase in bearing capacity with increasing depth is much more significant for G equal to 10 than for G equal to 0. In addition it can be seen that the smaller the angle φ, the greater the effect of increasing depth upon bearing capacity. For example, for $\phi = 20^{o}$, an increase in the depth to breadth ratio from 0 to 0.2 increases the bearing capacity by 40 percent. For $\phi = 40^{o}$, however, the bearing capacity increases by only 20 percent.

In Fig. 7 bearing capacity of shallow rough footings is plotted against values of G ranging from 0.1 to 10, for 5 values of D/B and for ϕ ranging from 10^{o} to 30^{o}. In Fig. 8 similar charts are presented for deep footings for depth to breadth ratios up to 5.

It was pointed out earlier that base friction can have a significant effect upon the bearing capacity of surface footings. However, the analysis presented here indicates that the significance of base friction is greatly reduced for deep footings. Fig. 9 shows the relationship between bearing capacity and depth for both a perfectly

smooth and a perfectly rough base. In Fig. 9, G is equal to 1. The figure shows clearly that as the depth increases the difference in bearing capacities of a rough and smooth footing diminishes. In fact it can be seen that at some depth the bearing capacities of a smooth and rough footing become identical.

The bearing capacity of rough footings is governed by the Prandtl mechanism. For smooth footings the Hill mechanism governs until the two curves intersect. For greater depths the Prandtl mechanism gives a smaller upper bound than does the Hill mechanism.

7. COMPARISON OF RESULTS WITH EXISTING SOLUTIONS

Since the upper bound technique of limit analysis gives only an approximate solution to the bearing capacity problem, some measure of the accuracy of the solutions must be determined. Hence, the present solutions will first be compared to slip-line solutions, followed by a comparison with limit equilibrium solutions.

Cox [2] has published slip-line solutions for the bearing capacity of a smooth surface footing. In that work, values of G ranging from 0 to 10 and ϕ ranging from 0° to 40° are considered. In addition Spencer [19] has published approximate solutions for the same problem using a perturbation technique, where the first term of the perturbation expansion corresponds to the solution for a weightless soil.

Cox's solutions, Spencer's solutions, and the limit analysis solutions developed here are tabulated in Table 1. It is noted that limit analysis gives the exact solution when G is equal to zero. From examination of the tabular results it can be seen that the error associated with the limit analysis solutions increases as G and ϕ increase. A brief discussion of limit analysis solutions for $G = \infty$ (cohesionless soil) is presented in Appendix 2. The error discussed here is referred to the slip-line solutions of Cox.

For G equal to 10 and ϕ equal to 40°, the upper bound limit analysis method overestimates the slip-line solution by 40 percent. For G less than 5 and ϕ less than 40°, the error can be expected to be less than 25 percent. As was mentioned earlier, however, the values of G can normally be expected to range from 0.1 to 1, and within this range the maximum error in the limit analysis solutions is less than 9 percent.

It is of interest to compare the results of Spencer with the limit analysis solutions. The two methods give nearly identical results with the limit analysis solutions lying slightly closer to the slip-line solutions. One might interpret Spencer's technique as an upper bound approach in which the kinematically admissable velocity field is that of a weightless soil [2]. The velocity field used here resembles closely that of a weightless soil, however, the size of various zones (rigid body zones and a radial shear zone) are varied in order to minimize the load, thus accounting for the slight improvement over Spencer's solution. The authors found that they could duplicate

Spencer's results by using the velocity field for a weightless soil.

To date there have been so slip-line solutions published for a rough surface footing or a rough or smooth subsurface footing bearing on a cohesive soil with weight. However, the success of the limit analysis approach in predicting the bearing capacity of smooth surface footings leads the authors to believe that it will be equally successful in predicting the bearing capacity of subsurface footings as well as rough surface footings.

Some limit analysis and limit equilibrium solutions for surface and subsurface footings are tabulated in Table 2. The limit analysis solutions are for a perfectly rough footing base.

The solutions described by Terzaghi [21] neglect the strength of soil above the footing base. Meyerhof's solutions for surface footings are obtained from Ref. 13 while those for a subsurface footing are obtained from Ref. 12. The conversion from D/B to Meyerhof's angle "β" (same as the angle β used here in the Prandtl and Hill geometries) was determined from a chart on page 422 in Ref. 15. Although Meyerhof's method is equally applicable for a friction angle of 10° as for other friction angles, the chart mentioned above does not include friction angles less than 20°. It is for this reason that Meyerhof's solutions for a friction angle of 10° are not included in the table. The solutions ascribed to Hansen were obtained from Ref. 9 and incorporate the so-called depth factors.

Considering first the two surface footing cases, it can be seen that the limit analysis solutions exceed all the limit equilibrium

solutions. For the values of ϕ and G under consideration, the limit analysis solutions probably lie quite close to the true solutions. The difference between the limit analysis and limit equilibrium solutions can probably be attributed to the use of superposition in all three limit equilibrium solutions.

The solutions of Meyerhof and the limit analysis solutions agree remarkably well for subsurface footings. The two methods use somewhat similar failure mechanisms and both include the strength of soil above the footing base. It can also be seen that the solutions of Hansen agree fairly well with the limit analysis results, with the differences tending to increase with increasing depth. The Terzaghi solutions presented here differ considerably from the other solutions. This is not surprising since the Terzaghi results do not include soil strength above the footing base.

8. SUMMARY AND CONCLUSIONS

It has been shown that the upper bound technique of limit analysis can predict bearing capacities of cohesive ponderable soils with internal friction to within a reasonable degree of accuracy, for ϕ ranging from 0° to 40° and G ranging from 0 to 5. At the least, it can be said that the results compare favorably with existing limit equilibrium solutions.

The most forceful argument for the adoption of the proposed method is the fact that its rational basis allows it to be conveniently extended to more complex bearing capacity problems. For example, the

limit analysis method could be adopted to the solution of layered soils. The method could be more generally useful to solve the three-dimensional bearing capacity problem where exact solutions of the equations of plasticity are all but impossible except for the most elementary of problems.

APPENDIX 1

References

1. Chen, W. F., "Soil Mechanics and Theorems of Limit Analysis", Journal of the Soil Mechanics and Foundations Division, ASCE, Vol. 95, SM2, March 1959, pp. 493-518.

2. Cox, A. D., "Axially Symmetric Plastic Deformation in Soils-II-Indentation of Ponderable Soils", International Journal of Mechanical Sciences, Vol. 4, 1962, pp. 371-380.

3. De Josselin De Jong, G., "Graphical Method for the Determination of Slip-Line Fields in Soil Mechanics", (Dutch), Ingenieur, Vol. 69, No. 29, July 1957, pp. 61-65.

4. Drucker, D. C., "Coulomb Friction, Plasticity, and Limit Loads", Journal of Applied Mechanics, Vol. 21, No. 1, March 1954, pp. 71-74.

5. Drucker, D. C. and Prager, W., "Soil Mechanics and Plastic Analysis or Limit Design", Quarterly of Applied Mathematics, Vol. 10, No. 2, July 1952, pp. 157-165.

6. Drucker, D. C., Prager, W. and Greenberg, H. J., "Extended Limit Design Theorems for Continuous Media", Quarterly of Applied Mathematics, Vol. 9, No. 4, January 1952, pp. 381-389.

7. Graham, J. and Stuart, J. C., "Scale and Boundary Effects in Foundation Analysis", Journal of the Soil Mechanics and Foundations Division, ASCE, Vol. 97, No. SM11, November 1971, pp. 1533-1548.

8. Hansen, B. and Christensen, N. H., Discussion of "Theoretical Bearing Capacity of Very Shallow Footings", by L. A. Larkin, Journal of the Soil Mechanics and Foundations Division, ASCE, Vol. 95, No. SM6, November 1969, pp. 1586-1572.

9. Hansen, J. Brinch, "A General Formula for Bearing Capacity", Bulletin No. 11, The Danish Geotechnical Institute, 1961.

10. Lundgren, H. and Mortensen, K., "Determination by the Theory of Plasticity of the Bearing Capacity of Continuous Footings on Sand", Proceedings, Third International Conference on Soil Mechanics and Foundation Engineering, Vol. 1, 1953, pp. 409-412.

11. Lysmer, J., "Limit Analysis of Plane Problems in Soil Mechanics", Journal of the Soil Mechanics and Foundations Division, ASCE, Vol. 96, SM4, July 1970, pp. 1311-1334.

12. Meyerhof, G. G., "The Ultimate Bearing Capacity of Foundations", Geotechnique, Vol. 2, 1951, pp. 301-332.

13. Meyerhof, G. G, "Influence of Roughness of Base and Ground-Water Conditions on the Ultimate Bearing Capacity of Foundations", Geotechnique, Vol. 5, No. 3, September 1955, pp. 227-242.

14. Prandtl, L., "Uber Die Haerte Plastischer Korper", Nachrichten Von Der Koeniglichen Gesellschaft Der Wissenschaften Zu Geottingen, Mathematisch-physikalische Klasse, 1920, pp. 74-85.

15. Scott, R. F., "Plastic Equilibrium States in Soil", Principles of Soil Mechanics, Addison-Wesley Publishing Company, Inc., Reading, Massachusetts, 1963, p. 422.

16. Shield, R. T., "Mixed Boundary Value Problems in Soil Mechanics", Quarterly of Applied Mathematics, Vol. 11, No. 1, April 1953, pp. 61-75.

17. Shield, R. T., "Plastic Potential Theory and the Prandtl Bearing Capacity Solution", Journal of Applied Mechanics, Vol. 21, No. 2, June 1954, pp. 193-194.

18. Sokolovskii, V. V., Statics of Granular Media , Pergamon Press, New York, 1965.

19. Spencer, A. J. M., "Perturbation Methods in Plasticity - III Plane Strain of Ideal Soils and Plastic Solids with Body Forces", Journal of the Mechanics and Physics of Solids, Vol. 10, April/June 1962, pp. 165-177.

20. Terzaghi, K., "Theoretical Soil Mechanics", John Wiley and Sons, Inc., 1943.

21. Terzaghi, K. and Peck, R. B., "Plastic Equilibrium in Soils", Soil Mechanics in Engineering Practice, 2nd ed., John Wiley and Sons, Inc., 1967, pp. 219-213.

APPENDIX 2

Bearing Capacity of Cohesionless Soils

The mechanism shown in Fig. 10a will be referred to here as "Prandtl 2". It differs from the conventional Prandtl mechanism only insofar as an additional rigid body zone has been introduced (zone BHC). Another mechanism, called "Prandtl 3", is shown in Fig. 10b. It resembles closely the conventional Prandtl mechanism, however, the shear zone, BCD, is now bounded by a circular arc. The velocity of any radial line of the shear zone is uniform. The velocity vector is no longer perpendicular to the radial line but rather makes an angle of ϕ with a normal to the radial line.

Slip-line solutions for perfectly rough and perfectly smooth surface footings bearing on cohesionless soils ($G = \infty$) have been presented by Lundgren and Mortensen [10], Hansen and Christensen [8] and Graham and Stuart [7] among others. The results of Hansen and Christensen, as well as the limit analysis solutions obtained from the various mechanisms, are presented in Table 3. The results for "Prandtl 1" were obtained from the mechanism shown in Fig. 1.

As can be seen in Table 3, the limit analysis solutions exceed the slip-line solutions by 50 to 100 percent. It can also be observed that the limit analysis solutions can be improved somewhat by adding additional rigid bodies and using a modified shear zone.

It should be noted, however, that the slip-line solutions discussed here are not complete and hence are not necessarily true

solutions. The slip-line solutions may not, in fact, be upper bounds since they have never been integrated to yield a kinematically admissible velocity field. Nevertheless, these slip-line solutions probably represent the best solutions generated to date.

APPENDIX 3

Notation

The following symbols are used in this paper:

B, D	= width and depth of footing
c	= cohesive strength
D	= rate of internal energy dissipation
G	= $\gamma B/2c$
N_γ	= bearing capacity factor
q_o	= average bearing pressure at failure
r_o	= initial radius of radial shear zone
V	= velocity at arbitrary point in the radial shear zone
V_o	= initial velocity of radial shear zone
V_1	= velocity of wedge below footing
V_3	= velocity of zone BDEF
W	= rate of external work done by weight of radial shear zone
α	= defined by Eqs. 11,12 and 13
β, ξ, η, ζ	= angular parameters of mechanisms
γ	= weight density of soil
δ	= friction angle between footing base and adjacent soil

θ = angular coordinate of radial shear zone

Θ = angle subtended by radial shear zone

ϕ = internal friction angle of soil

TABLE 1 BEARING CAPACITIES (q_o/c) OF A SMOOTH SURFACE FOOTING

ϕ	G = 0.			G = .1			G = 1.0			G = 10.0		
	Cox	Spencer	Limit Analysis	Cox	Spencer	Limit Analysis	Cox	Spencer	Limit Analysis	Cox	Spencer	Limit Analysis
0^o	5.14	5.14	5.14	5.14	5.14	5.14	5.14	5.14	5.14	5.14	5.14	5.14
10^o	8.34	8.35	8.35	8.42	8.42	8.42	9.02	9.07	9.05	13.6	--	14.4
20^o	14.8	14.8	14.8	15.2	15.2	15.2	17.9	18.3	18.1	37.8	--	43.4
30^o	30.1	30.1	30.1	31.6	31.7	31.7	42.9	45.3	44.3	127.	--	159.
40^o	75.3	75.3	75.3	83.0	83.5	83.4	139.	157.	151.	574.	--	786.

TABLE 2 LIMIT ANALYSIS AND LIMIT EQUILIBRIUM SOLUTIONS FOR ROUGH FOOTINGS

ϕ	Geometry and Material Constants						Bearing Capacity pounds per square foot			
	c, pounds per square foot	B, feet	D, feet	γ, pounds per cubic foot	G	D/B	Limit Anal.	J. Brinch Hansen	Terzaghi	Meyerhof
10^{o}	1000	3	0	100	.15	0	8,560	8,370	8,000	8,000
30^{o}	500	10	0	100	1.0	0	29,100	24,100	23,000	23,000
10^{o}	1000	3	1.5	100	.15	.5	10,400	10,200	8,380	--
30^{o}	500	10	5	100	1.0	.5	41,800	37,400	32,000	41,000
10^{o}	1000	3	3	100	.15	1.0	12,100	11,100	8,750	--
30^{o}	500	10	10	100	1.0	1.0	56,200	51,100	41,000	54,500
30^{o}	500	10	20	100	1.0	2.0	88,800	81,700	59,000	82,300
30^{o}	500	10	50	100	1.0	5.0	210,000	183,000	113,000	207,000

TABLE 3 BEARING CAPACITY FACTORS FOR SURFACE FOOTINGS

ϕ	Rough Footing, $N_\gamma = 2q_o/\gamma B$				Smooth Footing, N_γ	
	Slip-line, Hansen & Christensen	Limit Analysis			Slip-line, Hansen & Christensen	Limit Analysis, Hill Mechanism
		Prandtl 1	Prandtl 2	Prandtl 3		
15^o	1.2	2.5	2.3	2.1	.7	1.2
20^o	2.9	5.9	5.2	4.6	1.6	2.7
25^o	7.0	12.0	11.4	10.9	3.5	5.9
30^o	15.0	27.0	25.0	31.5	7.5	13.0
35^o	35.0	60.0	57.0	138.0	18.0	29.0
40^o	85.0	150.0	141.0	1803.0	42.0	72.0

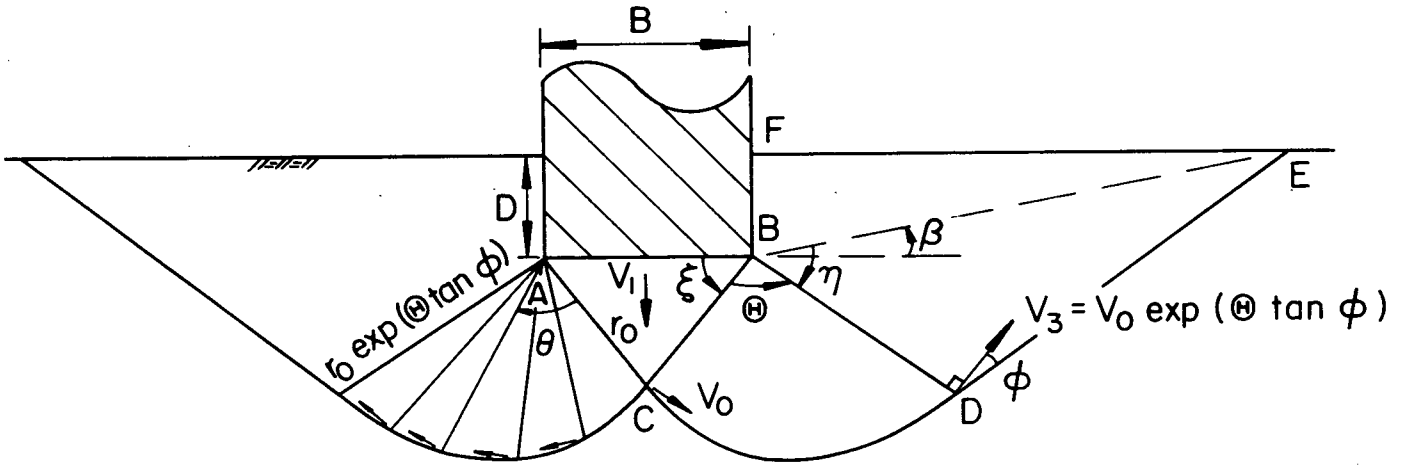

Fig. 1 "Prandtl" Mechanism

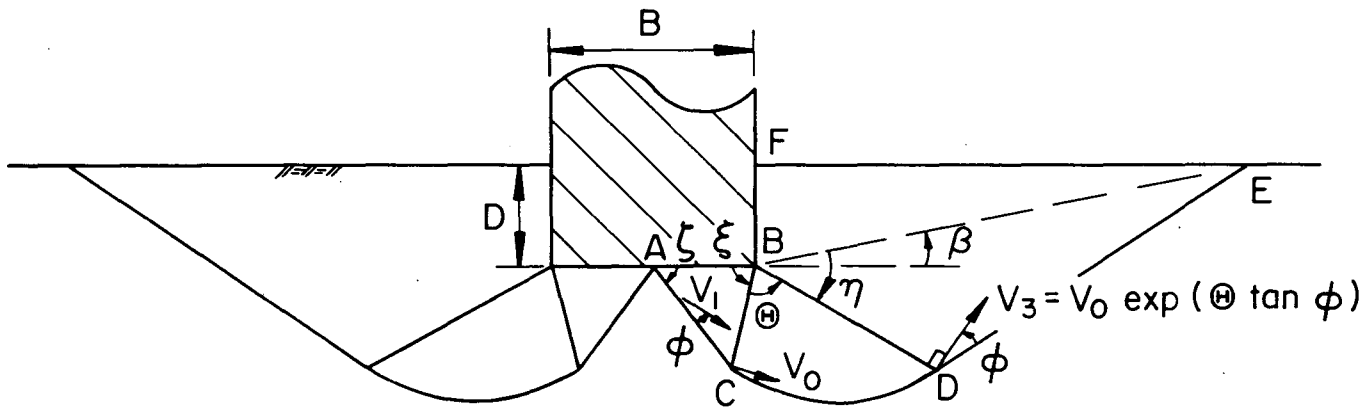

Fig. 2 "Hill" Mechanism

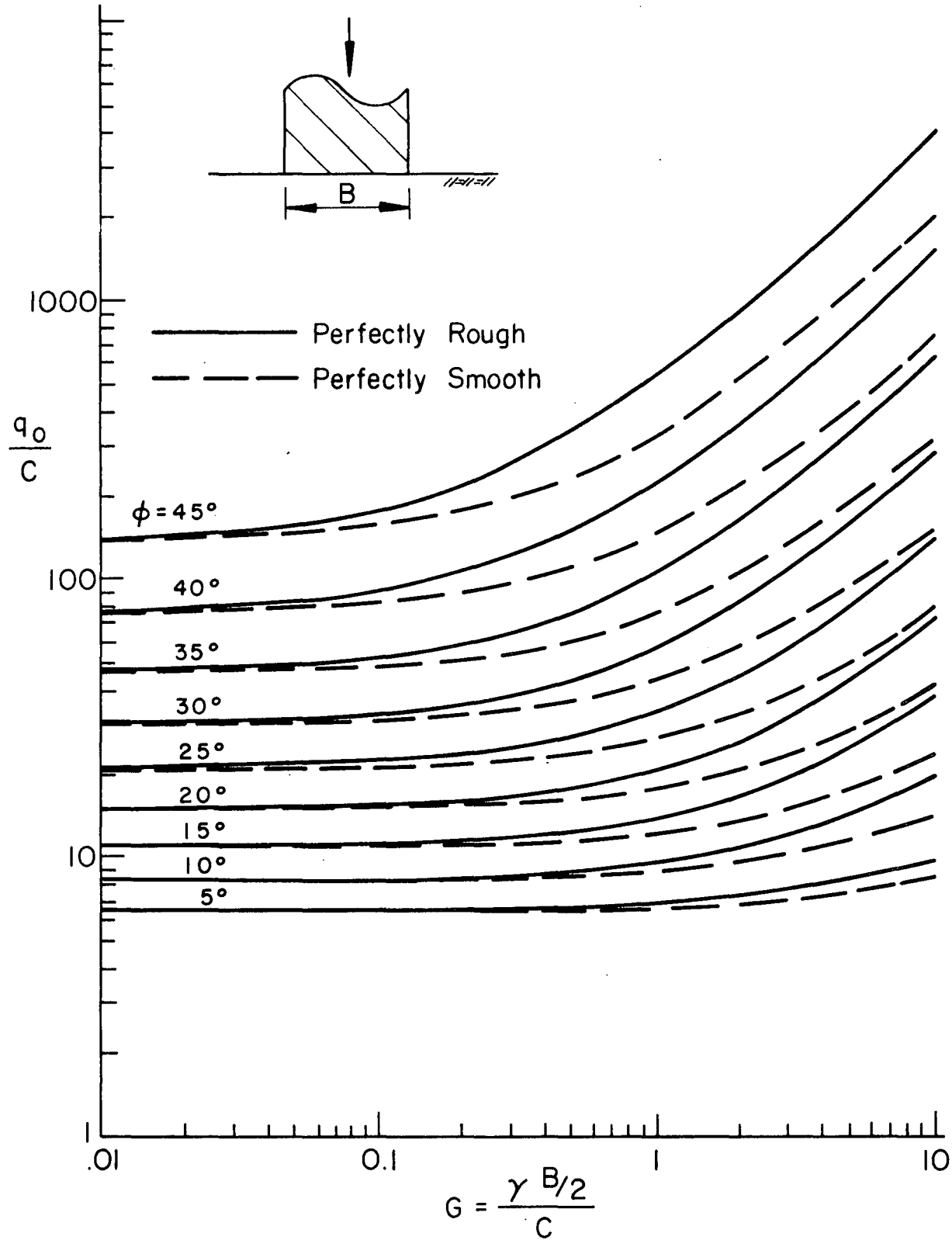

Fig. 3 Bearing Capacity of Surface Footings

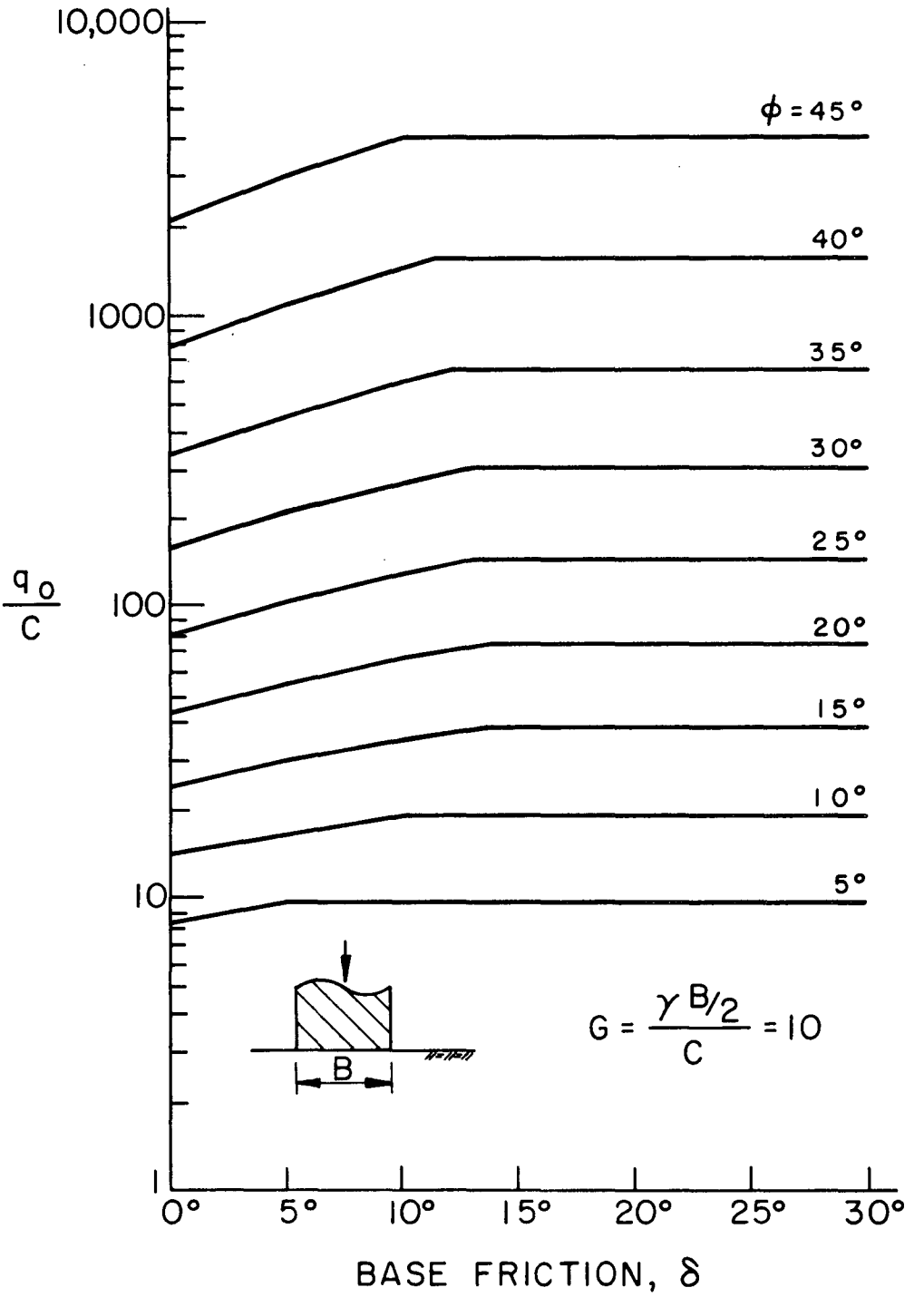

Fig. 4 Relationship Between Bearing Capacity and Base Friction

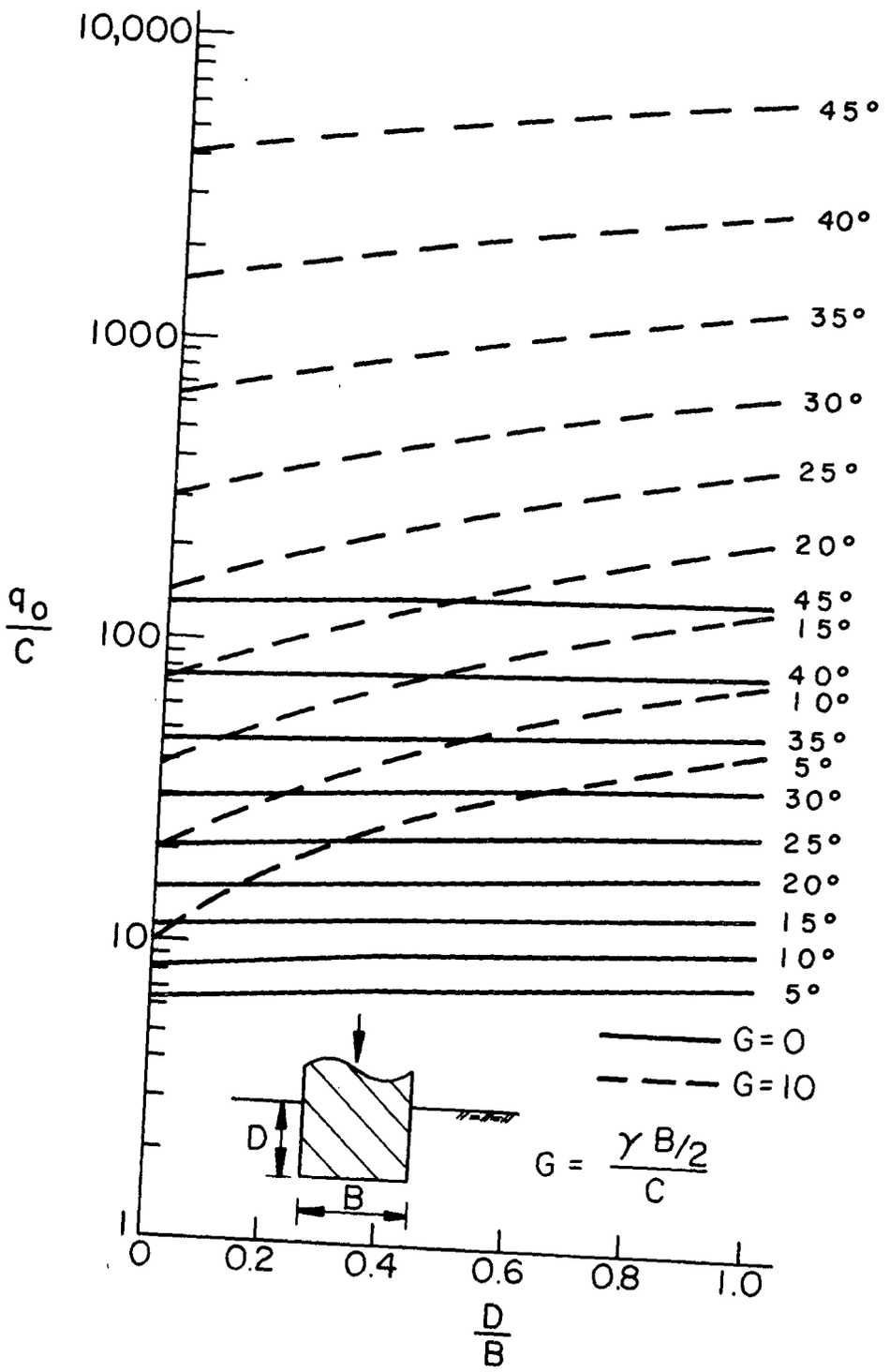

Fig. 5 Bearing Capacity of Shallow Footings

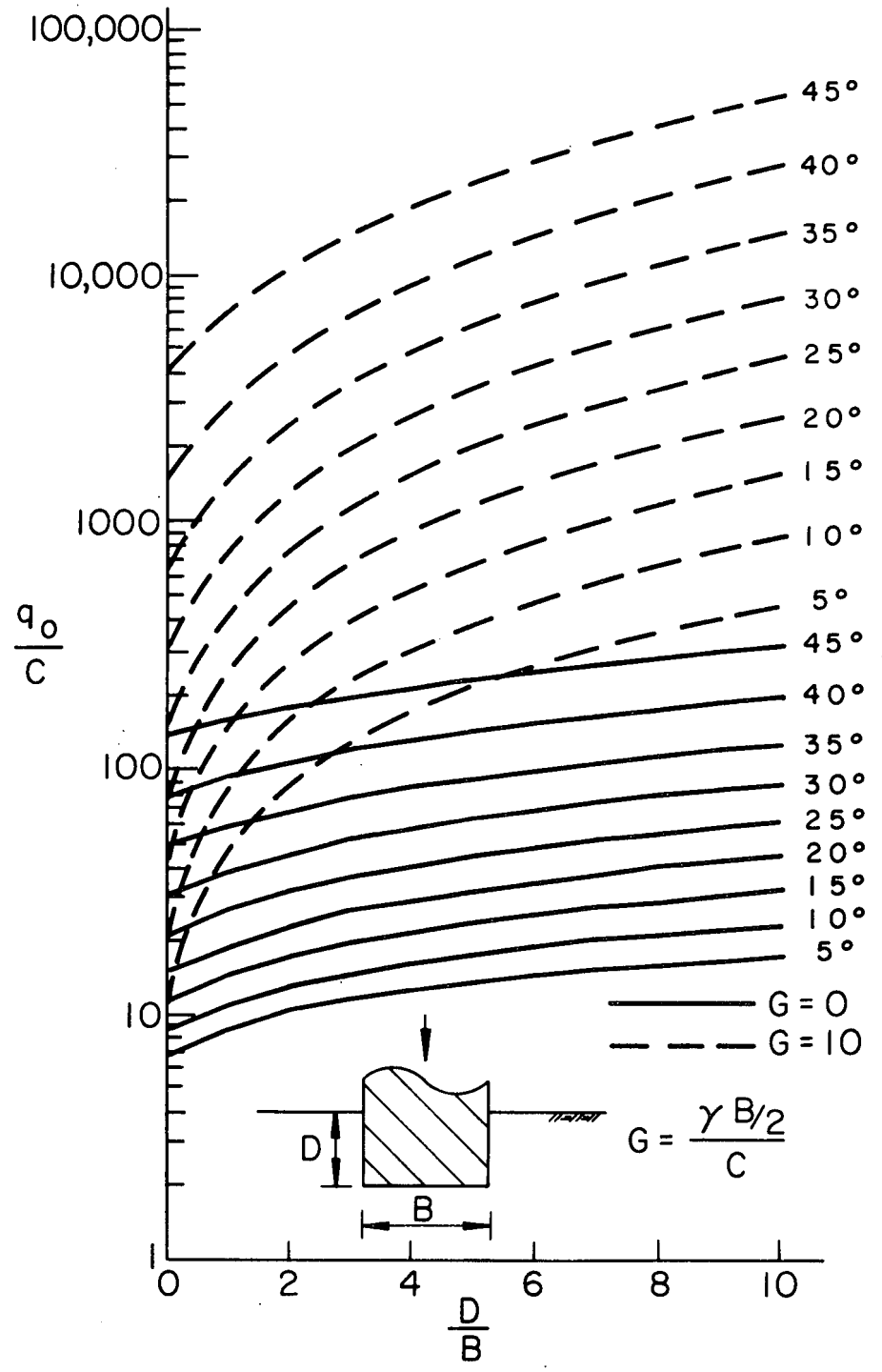

Fig. 6 Bearing Capacity of Deep Footings

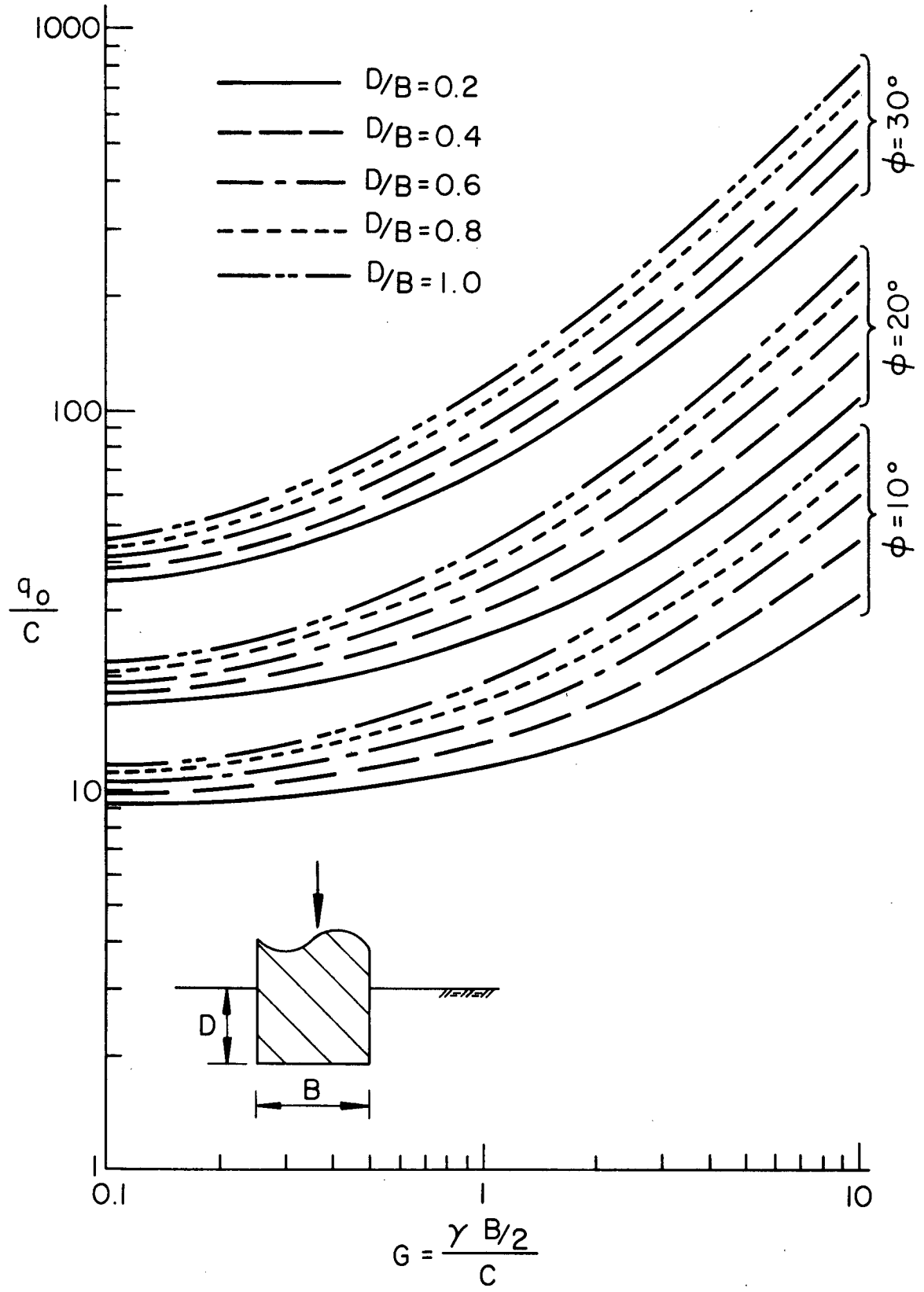

Fig. 7 Bearing Capacity of Shallow Rough Footings

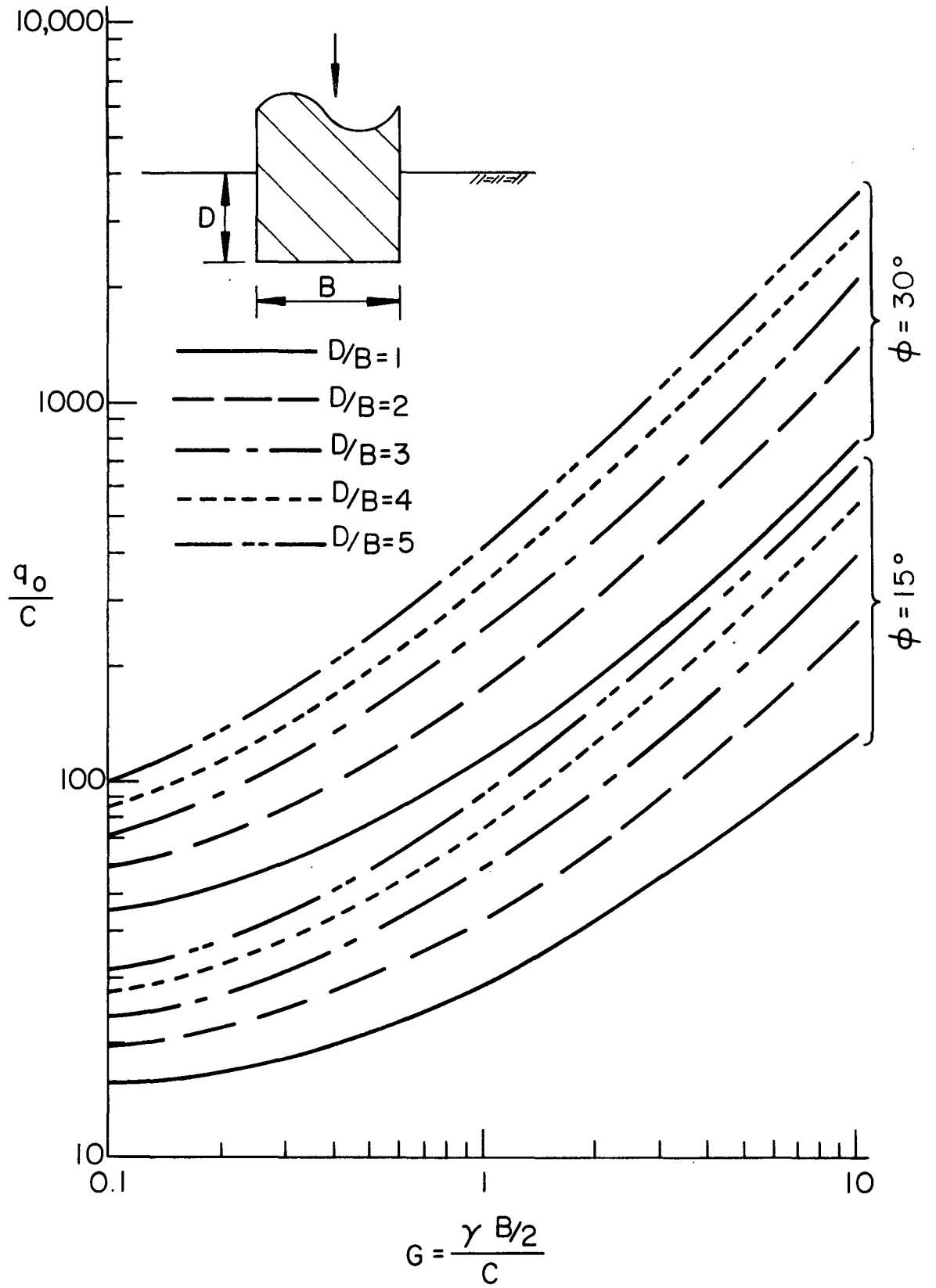

Fig. 8 Bearing Capacity of Deep Rough Footings

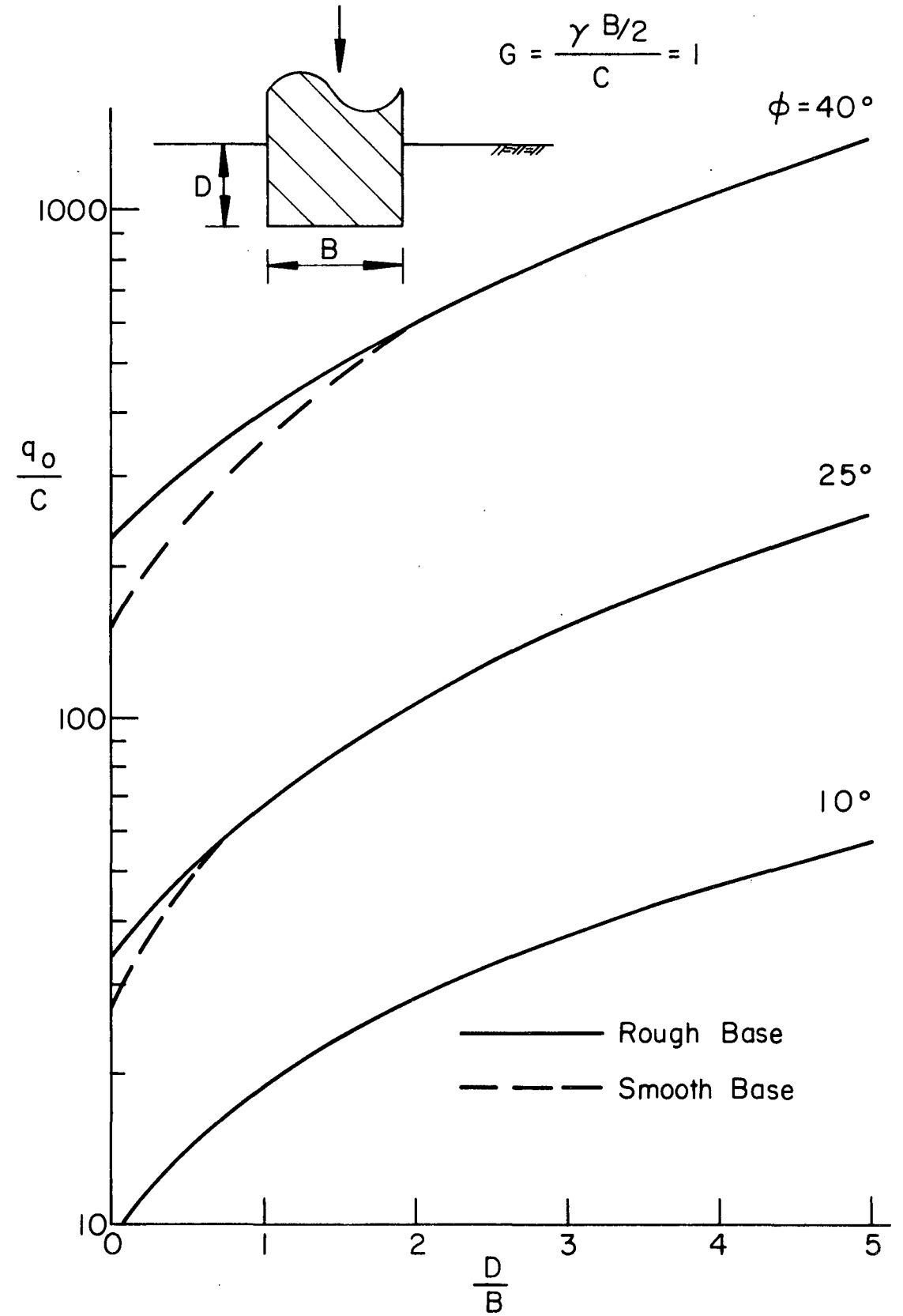

Fig. 9 Effect of Base Roughness on Bearing Capacity of Deep Footings

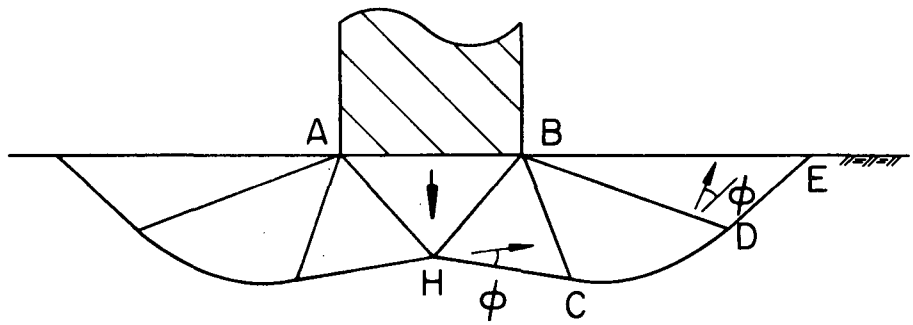

(a) "Prandtl 2" Mechanism

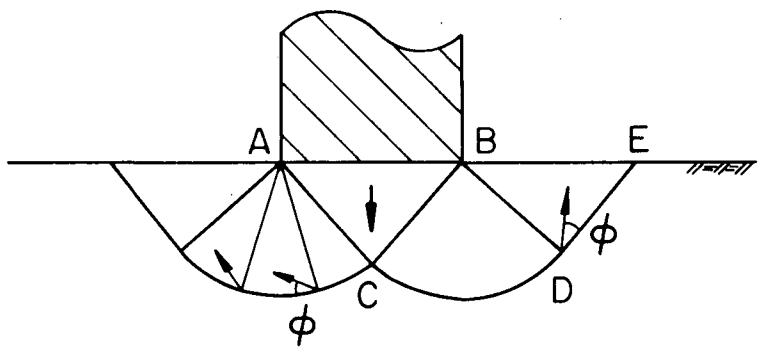

(b) "Prandtl 3" Mechanism

Fig. 10 Modified Prandtl Mechanisms

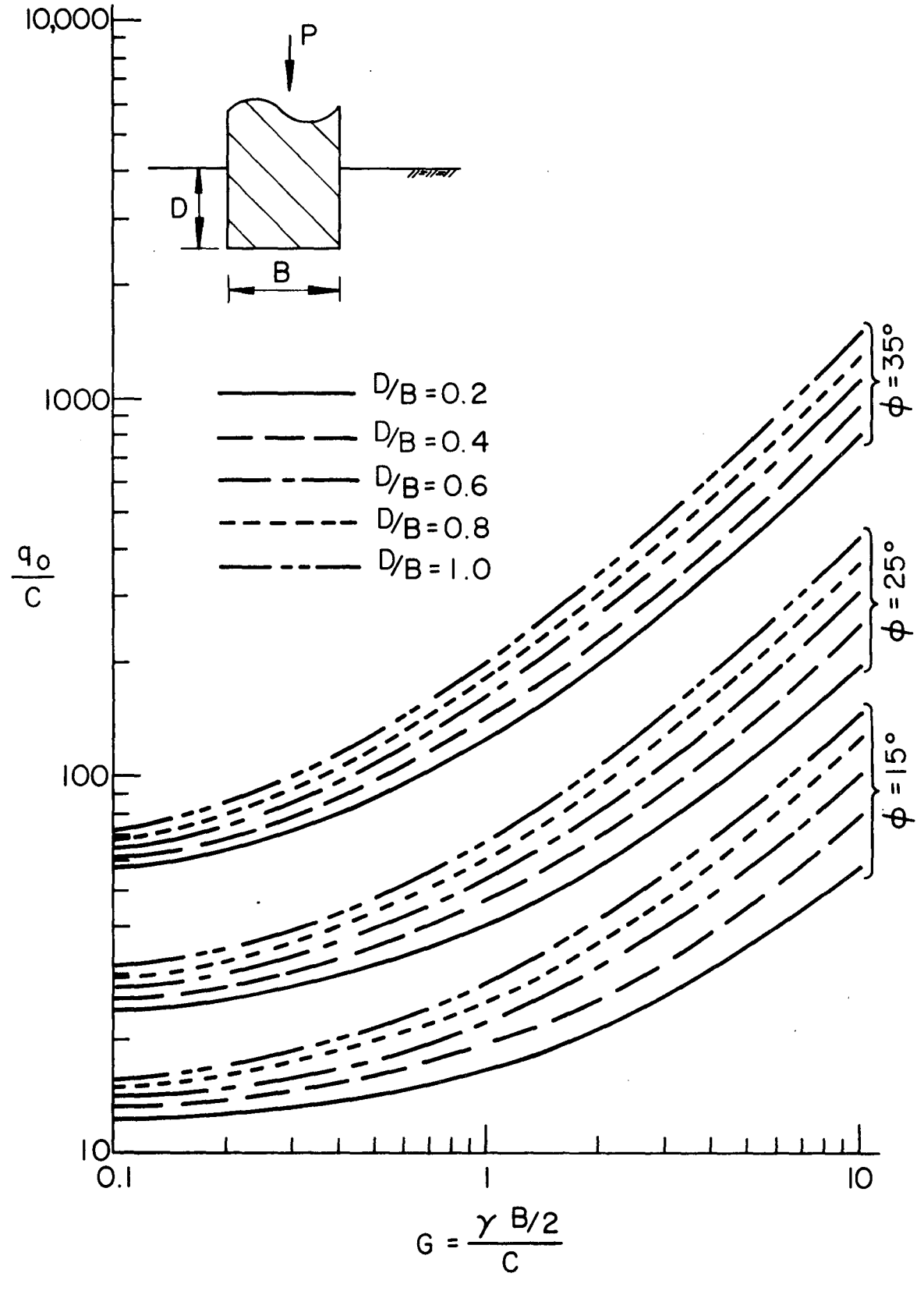

Fig. 11 Bearing Capacity of Shallow Rough Footings

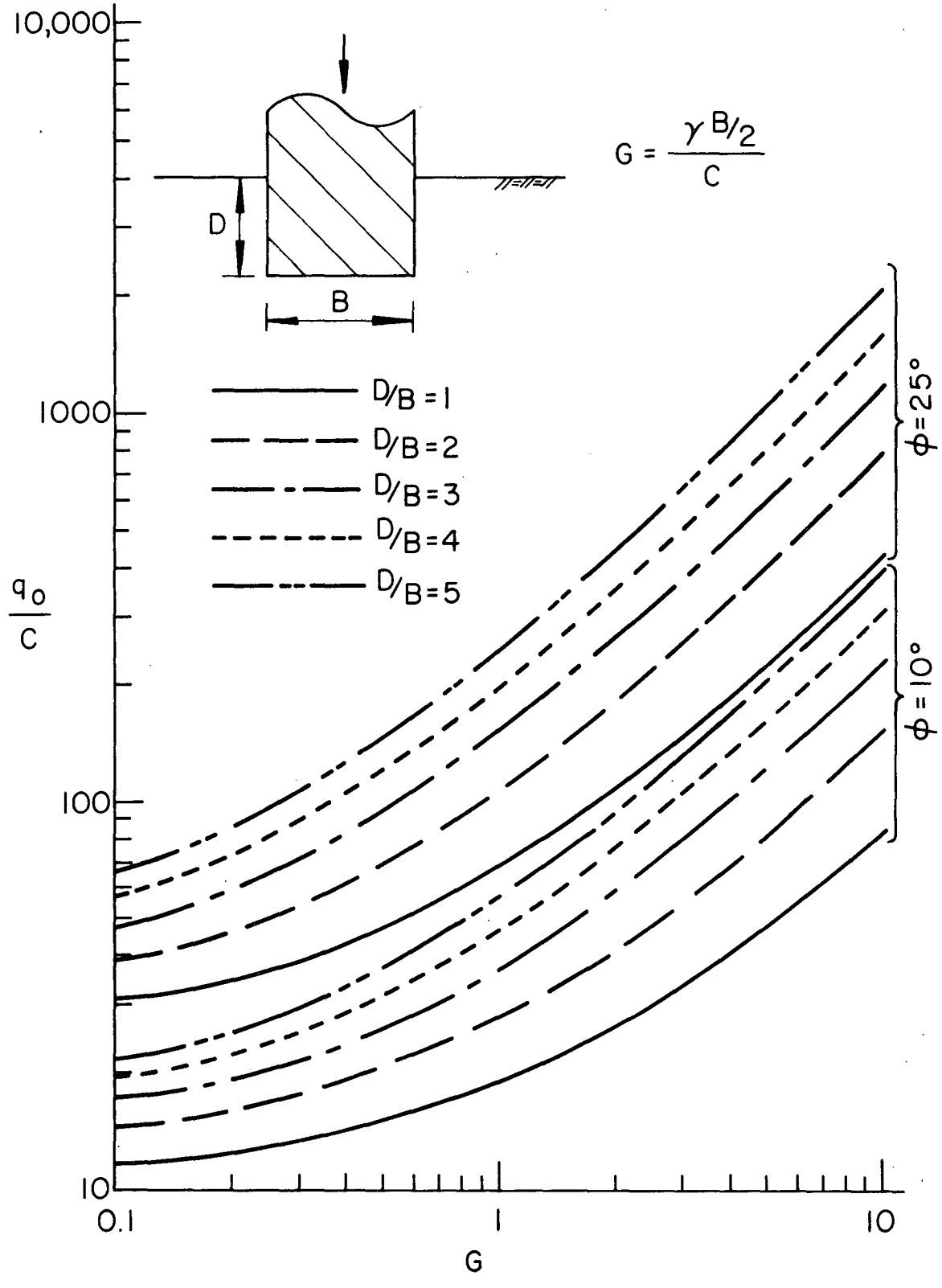

Fig. 12 Bearing Capacity of Deep Rough Footings

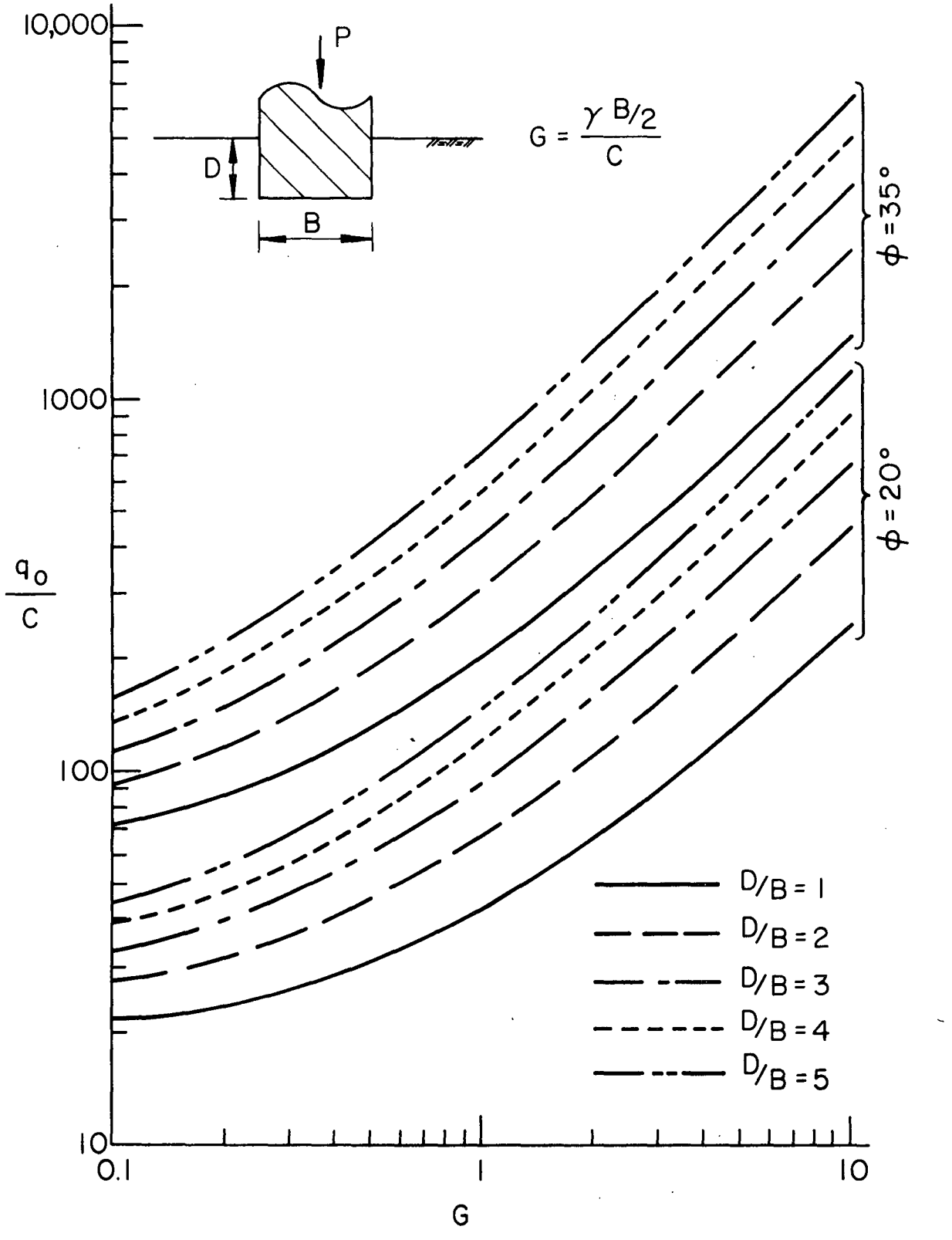

Fig. 13 Bearing Capacity of Deep Rough Footings

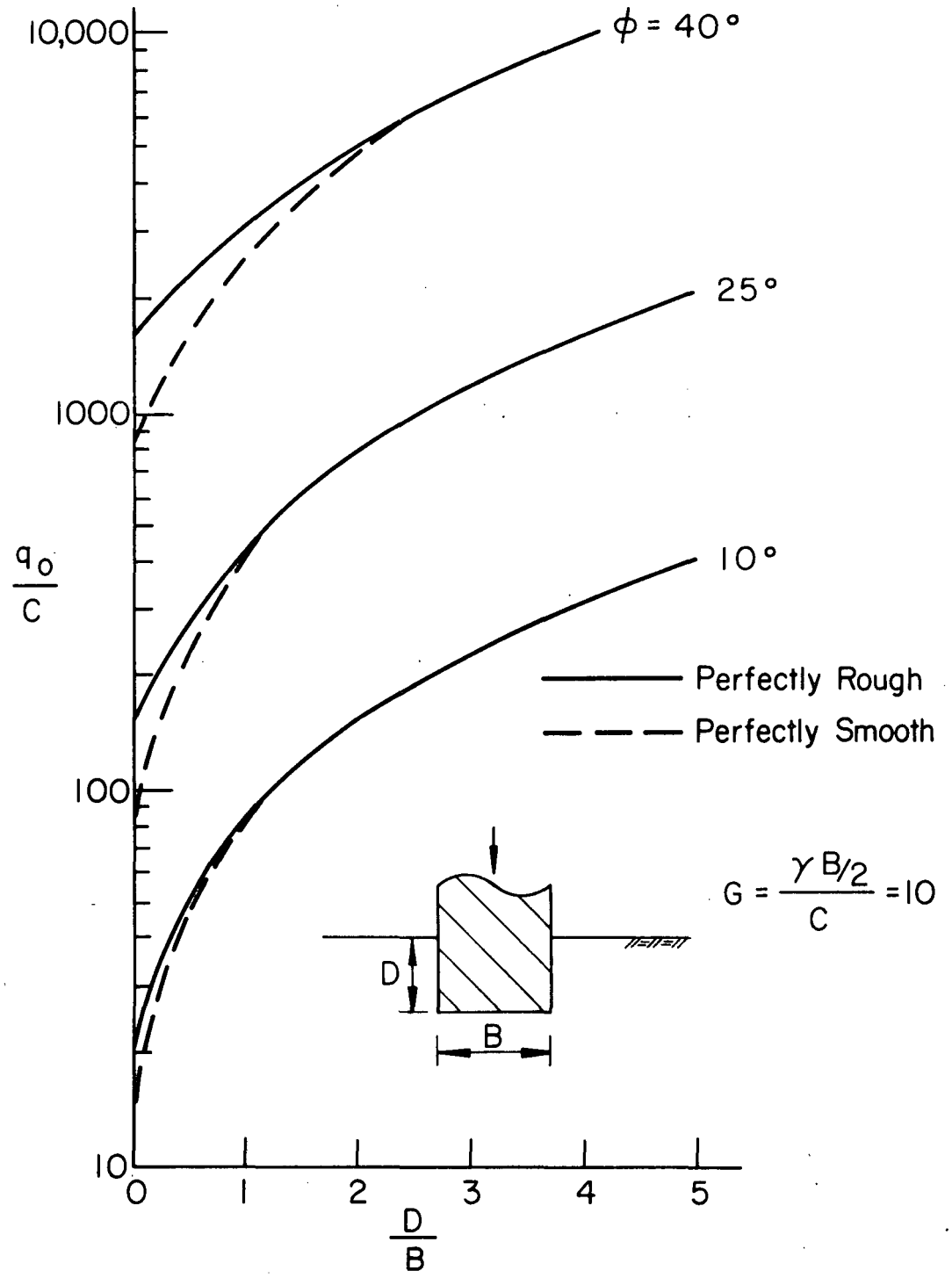

Fig. 14 Effect of Base Roughness on Bearing Capacity of Deep Footings

ACKNOWLEDGEMENTS

The writers wish to acknowledge Misses S. Matlock and P. Raudenbush for typing the manuscript and Mrs. S. Balogh for preparing the drawings.